LETTERS • OPEN ACCESS

Vibrational energy transfer from photoexcited carbon nanotubes to proteins observed by coherent phonon spectroscopy

To cite this article: Tomohito Nakayama *et al* 2017 *Appl. Phys. Express* **10** 125101

View the article online for updates and enhancements.

Vibrational energy transfer from photoexcited carbon nanotubes to proteins observed by coherent phonon spectroscopy

Tomohito Nakayama[1]*, Shunsuke Yoshizawa[1], Atsushi Hirano[2], Takeshi Tanaka[2], Kentaro Shiraki[1], and Muneaki Hase[1]*

[1]Division of Applied Physics, Faculty of Pure and Applied Sciences, University of Tsukuba, Tsukuba, Ibaraki 305-8573, Japan
[2]Nanomaterials Research Institute, National Institute of Advanced Industrial Science and Technology (AIST),
Tsukuba Central 5, Tsukuba, Ibaraki 305-8565, Japan

*E-mail: s1720384@s.tsukuba.ac.jp; mhase@bk.tsukuba.ac.jp

Vibrational energy transfer from photoexcited single-wall carbon nanotubes (SWCNTs) to coupled proteins is a key to engineering thermally induced biological reactions, for example, in photothermal therapy. Here, we explored vibrational energy transfer from photoexcited SWCNTs to different adsorbed biological materials by means of a femtosecond pump–probe technique. We show that the vibrational relaxation time of the radial breathing modes in SWCNTs depends significantly on the structure of the coupled materials, that is, proteins or biopolymers, indicating that the vibrational energy transfer is governed by overlapping of the phonon densities of states of the SWCNTs and coupled materials.
© 2017 The Japan Society of Applied Physics

Energy transfer from mechanical modes to organic layers or specimens has been extensively examined because there is broad interest in efficient energy conversion problems.[1,2] In particular, one-dimensional and two-dimensional structures made from carbon atoms have shown great advantages for vivid applications in fundamental systems such as biological and semiconductor devices[3,4] because of their extremely high carrier mobility, high thermal conductivity, and rigid structure.[5] Carbon nanotubes (CNTs) are promising materials for fabricating nanomachines suitable for use in medical treatments[6] such as photothermal therapy. To realize this potential application, it is highly important to understand the behavior of proteins on CNTs. Although extensive efforts have been made to understand and control the attraction between CNTs and proteins, only limited knowledge of their physical and chemical properties under static conditions has been obtained.[7]

Single-wall CNTs (SWCNTs) are one of the most popular and fundamental carbon materials, and they have metallic or semiconducting properties[8] depending on the nanotube symmetry and diameter, which are specified by the chiral vector.[9] Frequency-domain spectroscopy revealed diameter-selective Raman scattering from the radial breathing modes (RBMs) in SWCNTs,[10,11] where the frequency of the RBMs depends on the inverse of the diameter. Moreover, Hertel et al. investigated the effects of the environment on the optical properties of SWCNTs. They found that the interactions between the SWCNTs and their environment depended on their diameter and exciton energy.[12] Recently retention of the antibacterial activity of proteins with the aid of SWCNTs was demonstrated.[7] In addition, hen egg-white lysozyme (LYZ) has been demonstrated to disperse SWCNTs, depending on the pH value.[13] However, little is known about the vibrational energy transfer between SWCNTs and proteins such as LYZ, particularly on femtosecond to picosecond time scales, at which phonon–phonon coupling may play a significant role. Understanding and controlling the vibrational energy transfer between SWCNTs and proteins (or biopolymers) will be highly relevant to engineering thermally induced biological reactions.
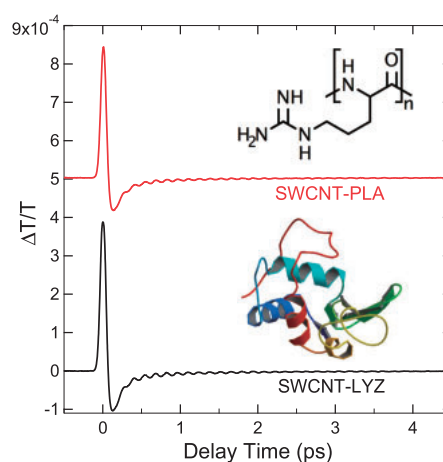

Fig. 1. Time-resolved transmission obtained for SWCNT-LYZ and SWCNT-PLA at room temperature. The inset shows schematics of the two absorbed molecules.

In this study, coherent vibrational motion of the RBMs in SWCNTs coupled with proteins or biopolymers was precisely measured on femtosecond time scales. We show that the relaxation dynamics of the coherent RBM depend on the coupled species, from which it is possible to gain new insights into vibrational energy transfer from photoexcited SWCNTs to coupled species. Here, we selected two types of cosolute, that is, LYZ and poly(L-arginine) (PLA), as materials interacting with SWCNTs to investigate their structural effects. Both of them have the ability to disperse SWCNTs, although these solutes have different structures. LYZ consists of 129 amino acid residues (molecular weight: 14,307) with a basic isoelectric point (pI = 11). The tertiary structure of LYZ in aqueous solution is highly stable, and it has secondary structures including the α-helix and β-sheet (Fig. 1 inset). On the other hand, PLA (molecular weight: >70,000) is made by polymerizing a basic amino acid, arginine ($pK_a = 12.5$) (Fig. 1 inset). As described below, we could observe differences in the dynamics of the coherent RBM phonon between these biomaterials, which are argued to originate from their structures and thereby their phonon densities of states (PDOSs).

The samples of SWCNTs were produced via the high-pressure catalytic CO decomposition process.[14] Hen egg-white LYZ and PLA were obtained from Sigma-Aldrich. The SWCNT-protein dispersions were prepared as described previously.[15] Briefly, a solution containing LYZ (0.2 mg/mL) or PLA (0.2 mg/mL) was mixed with SWCNT powder. Then the SWCNTs were dispersed by ultrasonication for 60 min at 18 °C using an ultrasonic processor. Finally, a highly dispersed SWCNT solution was obtained from the supernatant of the sample solution after ultra-centrifugation (210,000g for 30 min at 25 °C) using an ultra-centrifuge. In addition, a bundled SWCNT sample was also obtained from the supernatant of the dispersed solution after gentle centrifugation (16,100g for 1 min at 25 °C).

The transient transmission ($\Delta T/T$) of the samples, that is, SWCNTs dispersed by LYZ (SWCNT-LYZ) or by PLA (SWCNT-PLA), was measured in a 5-mm-thick quartz cell by employing the fast scanning delay method.[16] The pump and probe pulses (20 fs pulse duration; 830 nm wavelength; 80 MHz repetition rate) were focused on a 70-µm-diameter spot in the sample with a mutual angle of ≈10°. The pump pulse, which had a constant average power (40 mW), generated a carrier density of 4×10^{19} cm^{-3}; the probe power was less than 2 mW. Under the constant pump power and focused spot size, the pump fluence should be constant throughout the measurements, and therefore the effect of the excitation density on the vibrational relaxation dynamics, that is, the carrier-density-dependent carrier–phonon scattering, was negligible in the present study. The polarization of the two beams was linear with a mutual angle of 55° (the magic angle).[17]

The $\Delta T/T$ signals were recorded as a function of the pump–probe time delay, as shown in Fig. 1. A transient electronic response is observed just at zero time delay and is followed by coherent phonon oscillations due to the RBMs, whose frequency (ω_{RBM} in THz) depends inversely on the diameter of the SWCNTs (R_{CNT} in nm),[17]

$$\omega_{RBM} = 7.44/R_{CNT}. \qquad (1)$$

The transient electronic response appearing just at zero time delay corresponds to coherent arrangement of the SWCNT molecules induced by the electric field of the femtosecond laser pulse and is governed by the third-order non-linear susceptibility $\chi^{(3)}$ (Ref. 18). To subtract the transient electronic response, we fitted the time domain data (Fig. 1) with a double-exponential decay function. Subsequently, we subtracted the double-exponential decay function from the time-domain data. Thus, we obtained only the oscillatory parts of the time-domain signals (Fig. 2). A comparison of the $\Delta T/T$ signal obtained in the different systems, that is, SWCNT-LYZ and SWCNT-PLA, shows that the coherent phonon spectra are indeed different, indicating that the interaction between SWCNTs and biomaterials depends on their structures [Fig. 2(a)]. By using the Kataura plot, it is possible to derive the electronic states of the SWCNTs and hence to identify whether they are semiconducting or metallic. In our samples, the diameter of the SWCNTs has a range of 0.9–1.3 nm. Considering the photon energy (830 nm, i.e., 1.49 eV) and the broad bandwidth (≈50 nm, full width at half-maximum) of the laser used, the excitonic transitions around the critical point of S_{22} (the second-order semiconducting optical
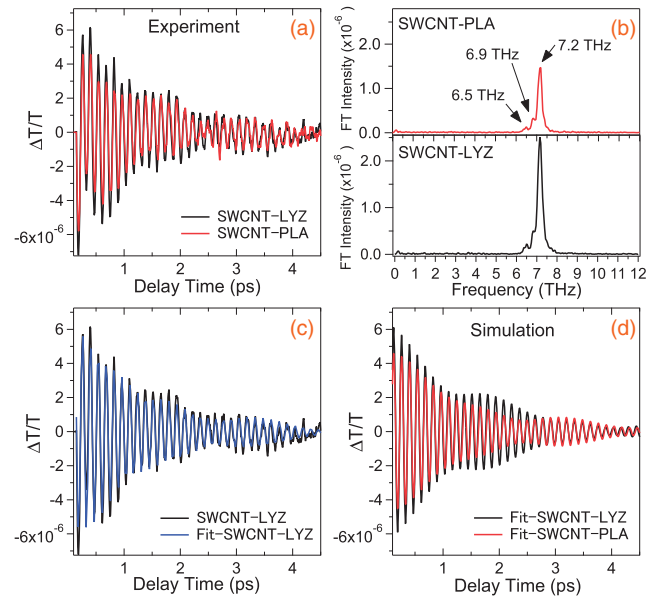

Fig. 2. (a) Coherent oscillation signals for SWCNT-LYZ (black) and SWCNT-PLA (red). (b) FT spectra obtained from the experimental time-domain data exhibited in panel (a). (c) Time-domain data of $\Delta T/T$ (black) and fitting data (blue) for SWCNT-LYZ. (d) Simulated data drawn using Eq. (2) with the parameters listed in Table I.

transition) are available at 800–900 nm (Ref. 19). We can thus conclude that the semiconducting SWCNTs are resonantly excited by impulsive stimulated Raman scattering.[20,21] Actually, the peaks at 6.5, 6.9, and 7.2 THz observed in the Fourier-transformed (FT) spectra [Fig. 2(b)] are assigned to 1.14-, 1.08-, and 1.03-nm-diameter tubes, respectively, on the basis of Eq. (1). Note that the chirality (n, m) of these modes can be (9, 7), (8, 7), and (12, 1) for the 1.14-, 1.08-, and 1.03-nm-diameter tubes, respectively.[22] The time-domain data were fitted to a linear combination of damped harmonic oscillators,

$$\Delta T/T = A_1 e^{-t/\tau_1} \cos(2\pi\nu_1 t + \phi_1)$$
$$+ A_2 e^{-t/\tau_2} \cos(2\pi\nu_2 t + \phi_2)$$
$$+ A_3 e^{-t/\tau_3} \cos(2\pi\nu_3 t + \phi_3), \qquad (2)$$

where A (A_1, A_2, A_3), τ (τ_1, τ_2, τ_3), ν (ν_1, ν_2, ν_3), and ϕ (ϕ_1, ϕ_2, ϕ_3) are the amplitude, relaxation time, frequency, and initial phase of the three coherent RBMs of the first ($\nu_1 = 6.5$ THz), second ($\nu_2 = 6.9$ THz), and third ($\nu_3 = 7.2$ THz) modes, respectively. The time-domain data are well fitted to Eq. (2), as shown in Fig. 2(c), and the obtained fitting parameters are listed in Table I. By comparing the amplitude of the dominant RBM (7.2 THz) for the two biomaterials, we found that the initial vibrational amplitude for the SWCNT-LYZ system is ≈1.6 times larger than that for the SWCNT-PLA system [see Table I and Fig. 2(d)], which is ascribable mainly to the difference in the concentration of SWCNTs between these samples;[23] note that the absorbance of SWCNT-LYZ at an 810 nm peak after background subtraction was ≈2.1-fold higher than that of SWCNT-PLA (Fig. 3).

Here, we focus on the strongest RBM, at 7.2 THz, by extracting the vibrational energy transfer dynamics from the fitting results. Importantly, the vibrational relaxation time for SWCNT-LYZ (ca. 1.41 ps) at 7.2 THz was shorter than that for SWCNT-PLA (ca. 1.66 ps), suggesting that the vibra-

Table I. Fitting parameters obtained using Eq. (2). The values for ν were obtained from the peak frequencies in the FT spectra [Fig. 2(b)] and treated as constants during the fitting. The standard deviation of the coefficients was obtained during the fitting procedure using Igor Pro.

Sample	Mode	ν (THz)	$A \times 10^6$	τ (ps)	ϕ (deg)
	First	6.5	0.59 ± 0.05	2.16 ± 0.20	-109.1 ± 2.5
SWCNT-LYZ	Second	6.9	0.39 ± 0.04	3.76 ± 0.50	74.8 ± 3.2
	Third	7.2	6.38 ± 0.06	1.41 ± 0.01	23.4 ± 0.3
	First	6.5	0.54 ± 0.06	1.94 ± 0.22	-130.4 ± 3.4
SWCNT-PLA	Second	6.9	0.78 ± 0.08	2.00 ± 0.17	58.6 ± 2.9
	Third	7.2	4.03 ± 0.06	1.66 ± 0.03	18.5 ± 0.4

Fig. 3. Absorption spectra of SWCNT-LYZ (black) and SWCNT-PLA (red) dispersions. The inset shows the enlarged spectra normalized at 600 nm together with that of the bundled form of the SWCNT-PLA (green). M_{11} represents the first-order metallic optical transition, whereas S_{11}, S_{22}, and S_{33} represent the first-, second-, and third-order semiconducting optical transitions, respectively.[23]

tional energy transfer from the photoexcited SWCNTs to LYZ is faster than that from the SWCNTs to PLA for the 7.2 THz mode. These vibrational relaxation time constants are significantly shorter than those obtained for SWCNTs dispersed in sodium dodecyl sulfate (SWCNT-SDS) (ca. 2.04 ± 0.02 ps) (data not shown), which was consistent with the value reported in the previous study,[17] indicating that the vibrational relaxation time of the coherent RBM in the present complex systems was indeed changed by the adsorbed biomaterials. Although decay of the coherent RBM is generally accounted for by anharmonic phonon–phonon energy relaxation into underlying acoustic phonons,[17] this decay path depends only on the temperature, so that the change in the relaxation time observed in Fig. 2 at constant room temperature cannot be accounted for by the anharmonic phonon–phonon energy relaxation. Note that the total relaxation rate $1/\tau$ is the sum of the new path and the existing path (anharmonic phonon–phonon energy relaxation), $1/\tau = 1/\tau_{\text{anharmonic}} + 1/\tau_{\text{new}}$, where we will discuss the origin of the new path (τ_{new}) in detail below.

It should be noted also that LYZ is adsorbed onto the SWCNTs through hydrophobic and π–π interactions,[24] whereas PLA is adsorbed onto the SWCNTs through hydrophobic and van der Waals interactions and partially through π–π interaction between the guanidinium group of arginine and the SWCNT surfaces.[15] Because of the different adsorption mechanisms, the coverage of the SWCNTs will not be the same for the two types of cosolute. The difference in the coverage of the SWCNTs can be reflected in the difference in the carrier doping of the SWCNTs.[25] However, in terms of the carrier doping, the differences in the coverage will not affect the vibrational relaxation time of the SWCNTs, because we have already demonstrated that the carrier doping did not affect the relaxation time of the RBMs.[17]

Because SWCNTs dispersed in aqueous solution generally exist as debundled or bundled forms,[15] the change in the relaxation time might be associated with the intertube interactions. In fact, the effects of bundling on the phonon relaxation have been examined using a SWCNT film and SWCNT solution for the G mode[26] as well as for the RBM,[27] revealing that bundling makes the phonon relaxation time shorter than that of individually dispersed SWCNTs. However, our samples used here were expected to be individually dispersed because they were collected from the supernatants after ultracentrifugation. To test this expectation, we measured the absorption spectra of the SWCNTs dispersed in solution as well as the bundled form (Fig. 3).
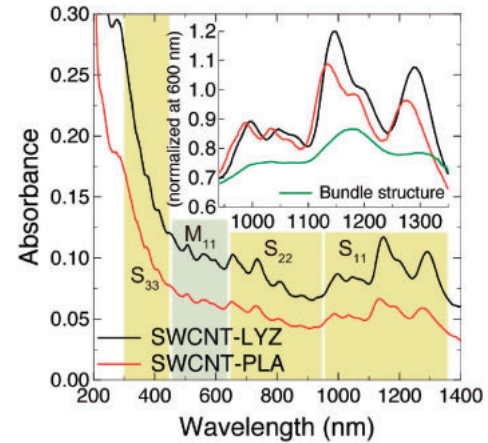
Although the absorption intensity of the S_{11} band was found to be slightly smaller and broader for SWCNT-PLA than for SWCNT-LYZ, the intensity of the S_{11} band was clearly stronger than that of the bundled form (see the inset of Fig. 3).[28] These results indicate that both SWCNT-LYZ and SWCNT-PLA were well dispersed. Thus, the decay-time shortening of the RBMs seen in the sample with LYZ can be explained mainly by energy transfer from the SWCNTs to LYZ and not by the bundling effect.

To further discuss the difference in the vibrational energy transfer observed in Fig. 2, the phonon–phonon coupling between the SWCNTs and biopolymers should be taken into account.[29,30] Recently, Li et al. observed anisotropic energy flow from proteins to ligands on albumin molecules using ultrafast infrared vibrational spectroscopy.[31] Efficient vibrational energy transfer was thought to occur through the connecting helix structures. In SWCNT-protein systems, similarly, favorable coupling would occur between the α-helix of the proteins and the SWCNTs.[32] Therefore, it is expected that vibrational energy transfer from the SWCNTs to the coupled LYZ might be more efficient than that from the SWCNTs to PLA, because only LYZ has the α-helix structure. We thus examine the vibrational energy transfer from SWCNTs to coupled biomaterials in terms of the phonon–phonon coupling on the basis of the PDOS.[29] The main peak in the PDOS at $\approx 240 \text{ cm}^{-1}$ ($= 7.2 \text{ THz}$) for LYZ[33] overlaps well the energy of the RBM (7.2 THz), whereas the overlap of the main peak ($\approx 250 \text{ cm}^{-1} = 7.5 \text{ THz}$) in the PDOS of PLA with the RBM (7.2 THz) is poor.[34] Therefore, there can exist resonant coupling between the RBM (7.2 THz) in the SWCNTs and the optical phonons in LYZ through the α-helix of the proteins, leading to efficient vibrational energy transfer. A possible scenario for the vibrational relaxation dynamics in the SWCNT-LYZ complex at 7.2 THz is schematically presented in Fig. 4, which shows that the vibrational amplitude of the SWCNTs readily decays by vibrational energy transfer to LYZ.

To further support our interpretation, we then focused on the vibrational relaxation time of the 6.9 THz mode. As shown in Table I, the relaxation time for SWCNT-PLA (ca.
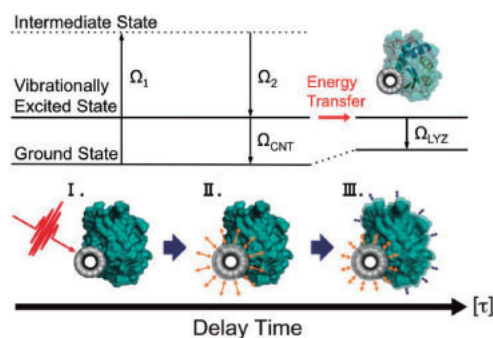
Fig. 4. Schematic dynamics of vibrational energy transfer from the SWCNTs to LYZ at 7.2 THz. The coherent RBM is excited via impulsive stimulated Raman scattering,[20] the spectra of which cover the excited phonon energy ($\Omega_{CNT} = \Omega_1 - \Omega_2$). Because the energy level of Ω_{CNT} and that of the phonon in LYZ (Ω_{LYZ}) overlap each other, effective energy transfer occurs. Three images in (I)–(III) illustrate the process of phonon–phonon coupling between the SWCNTs and LYZ as a function of the delay time. (I) The SWCNT is excited. (II) The coherent RBM in the SWCNT starts to oscillate. (III) The vibrational energy of the SWCNT's RBM propagates to the LYZ phonon mode.

2.00 ps) was significantly shorter than that for SWCNT-LYZ (ca. 3.76 ps), both of which are shorter than that of the 6.9 THz RBM in SWCNT-SDS (5.50 ± 0.17 ps) (data not shown). This result suggests that vibrational energy transfer from the photoexcited SWCNTs to PLA is faster than that from the SWCNTs to LYZ, which is consistent with the fact that the peak in the PDOS for PLA (≈ 230 cm^{-1} = 6.9 THz) overlaps well the energy of the RBM (6.9 THz).[34] Importantly, the difference in the relaxation times of the 7.2 THz mode for LYZ and PLA (i.e., 1.41 and 1.66 ps, respectively) is very small, whereas that of the 6.9 THz mode (i.e., 3.76 and 2.00 ps, respectively) is relatively large. A plausible reason for this lies in the natural linewidth of the PDOS inside a protein or biopolymer; specifically, the linewidth of the 240 cm^{-1} (7.2 THz) mode for LYZ (>10 cm^{-1})[33] is much broader than that of the 230 cm^{-1} (6.9 THz) mode for PLA (<10 cm^{-1}).[34] Therefore, the resonant energy transfer will be more pronounced for PLA than for LYZ at the respective peak positions in the PDOS. This could explain why the difference in the relaxation time is larger for the 6.9 THz mode. According to the above results and discussion, we concluded that the rate of phonon energy flow depends significantly on the PDOS of the biomaterials.

In summary, we explored the vibrational energy transfer between two different biomaterials and SWCNTs by means of the femtosecond transient transmission technique. The vibrational relaxation time of the RBMs changed dramatically depending on the PDOS of the coupled biomaterial. Our findings are particularly useful for designing a system for highly efficient phonon energy flow from photoexcited SWCNTs to biomaterials, and such vibrational energy transfer can be controlled by the PDOS originating in the structure of the coupled biomaterials.

1) M. D. Losego, M. E. Grady, N. R. Sottos, D. G. Cahill, and P. V. Braun, Nat. Mater. **11**, 502 (2012).
2) M. Hettich, K. Jacob, O. Ristow, M. Schubert, A. Bruchhausen, V. Gusev, and T. Dekorsy, Sci. Rep. **6**, 33471 (2016).
3) A. Modi, N. Koratkar, E. Lass, B. Wei, and P. M. Ajayan, Nature **424**, 171 (2003).
4) F. J. Wang, D. Kozawa, Y. Miyauchi, K. Hiraoka, S. Mouri, Y. Ohno, and K. Matsuda, Nat. Commun. **6**, 6305 (2015).
5) M. Zhang, T. Murakami, K. Ajima, K. Tsuchida, A. S. Sandanayaka, O. Ito, S. Iijima, and M. Yudasaka, Proc. Natl. Acad. Sci. U.S.A. **105**, 14773 (2008).
6) J. Kong, N. R. Franklin, C. Zhou, M. G. Chapline, S. Peng, K. Cho, and H. Dai, Science **287**, 622 (2000).
7) D. W. Horn, K. Tracy, C. J. Easley, and V. A. Davis, J. Phys. Chem. C **116**, 10341 (2012).
8) R. Saito, G. Dresselhaus, and M. S. Dresselhaus, *Physical Properties of Carbon Nanotubes* (Imperial College Press, London, 1998).
9) A. M. Rao, E. Richter, S. Bandow, B. Chase, P. C. Eklund, K. A. Williams, S. Fang, K. R. Subbaswamy, M. Menon, A. Thess, R. E. Smalley, G. Dresselhaus, and M. S. Dresselhaus, Science **275**, 187 (1997).
10) A. Jorio, R. Saito, J. H. Hafner, C. M. Lieber, M. Hunter, T. McClure, G. Dresselhaus, and M. S. Dresselhaus, Phys. Rev. Lett. **86**, 1118 (2001).
11) M. S. Dresselhaus, G. Dresselhaus, R. Saito, and A. Jorio, Phys. Rep. **409**, 47 (2005).
12) T. Hertel and G. Moos, Phys. Rev. Lett. **84**, 5002 (2000).
13) M. S. Strano, C. B. Huffman, V. C. Moore, M. J. O'Connell, E. H. Haroz, J. Hubbard, M. Miller, K. Rialon, C. Kittrell, S. Ramesh, R. H. Hauge, and R. E. Smalley, J. Phys. Chem. B **107**, 6979 (2003).
14) I. W. Chiang, B. E. Brinson, A. Y. Huang, P. A. Willis, M. J. Bronikowski, J. L. Margrave, R. E. Smalley, and R. H. Hauge, J. Phys. Chem. B **105**, 8297 (2001).
15) A. Hirano, T. Tanaka, H. Kataura, and T. Kameda, Chem.—Eur. J. **20**, 4922 (2014).
16) M. Hase, M. Kitajima, A. M. Constantinescu, and H. Petek, Nature **426**, 51 (2003).
17) K. Makino, A. Hirano, K. Shiraki, Y. Maeda, and M. Hase, Phys. Rev. B **80**, 245428 (2009).
18) Y.-R. Shen, *The Principle of Nonlinear Optics* (Wiley, New York, 1984).
19) H. Kataura, Y. Kumazawa, Y. Maniwa, I. Umezu, S. Suzuki, Y. Ohtsuka, and Y. Achiba, Synth. Met. **103**, 2555 (1999).
20) Y.-S. Lim, K.-J. Yee, J.-H. Kim, E. H. Hároz, J. Shaver, J. Kono, S. K. Doorn, R. H. Hauge, and R. E. Smalley, Nano Lett. **6**, 2696 (2006).
21) A. Gambetta, C. Manzoni, E. Menna, M. Meneghetti, G. Cerullo, G. Lanzani, S. Tretiak, A. Piryatinski, A. Saxena, R. L. Martin, and A. R. Bishop, Nat. Phys. **2**, 515 (2006).
22) S. V. Goupalov, B. C. Satishkumar, and S. K. Doorn, Phys. Rev. B **73**, 115401 (2006).
23) T. Tanaka, Y. Urabe, D. Nishide, and H. Kataura, Appl. Phys. Express **2**, 125002 (2009).
24) M. Calvaresi, S. Hoefinger, and F. Zerbetto, Chem.—Eur. J. **18**, 4308 (2012).
25) A. Hirano, T. Kameda, Y. Yomogida, M. Wada, T. Tanaka, and H. Kataura, ChemNanoMat **2**, 911 (2016).
26) Y. J. Lee, S. H. Parekh, J. A. Fagan, and M. T. Cicerone, Phys. Rev. B **82**, 165432 (2010).
27) Y. Honda, E. Maret, A. Hirano, T. Tanaka, K. Makino, and M. Hase, Appl. Phys. Lett. **102**, 222109 (2013).
28) M. J. O'Connell, S. M. Bachilo, C. B. Huffman, V. C. Moore, M. S. Strano, E. H. Haroz, K. L. Rialon, P. J. Boul, W. H. Noon, C. Kittrell, J. Ma, R. H. Hauge, R. B. Weisman, and R. E. Smalley, Science **297**, 593 (2002).
29) D. M. Leitner, Phys. Rev. Lett. **87**, 188102 (2001).
30) M. Hase, M. Kitajima, S. Nakashima, and K. Mizoguchi, Phys. Rev. Lett. **88**, 067401 (2002).
31) G. Li, D. Magana, and R. B. Dyer, Nat. Commun. **5**, 3100 (2014).
32) X. Hu, L. Hong, M. D. Smith, T. Neusius, X. Cheng, and J. C. Smith, Nat. Phys. **12**, 171 (2016).
33) A. V. Svanidze, I. L. Sashin, S. G. Lushnikov, S. N. Gvasaliya, K. K. Turoverov, I. M. Kuznetsova, and S. Kojima, Ferroelectrics **348**, 154 (2007).
34) P. Sharma, N. K. Misra, P. Tandon, and V. D. Gupta, J. Macromol. Sci., Part B **41**, 319 (2002).